Journal of Solid State Chemistry 182 (2009) 1055–1060

Contents lists available at ScienceDirect

Journal of Solid State Chemistry

journal homepage: www.elsevier.com/locate/jssc

Cobalt oxide hollow microspheres with micro- and nano-scale composite structure: Fabrication and electrochemical performance

Feifei Tao [a,b], Cuiling Gao [a], Zhenhai Wen [c], Qiang Wang [c], Jinghong Li [c], Zheng Xu [a,*]

[a] State Key Laboratory of Coordination Chemistry, Laboratory of Solid State Microstructures, School of Chemistry and Chemical Engineering, Nanjing University, Nanjing 210093, PR China
[b] School of Chemistry and Chemical Engineering, Shaoxing University, Shaoxing 312000, PR China
[c] Department of Chemistry, Qinghua University, Beijing 100084, PR China

ARTICLE INFO

Article history:
Received 25 August 2008
Received in revised form
15 January 2009
Accepted 26 January 2009
Available online 5 February 2009

Keywords:
Cobalt oxide
Hollow microspheres
Composite structure
Self-assembly
Electrochemical performance

ABSTRACT

Co_3O_4 hollow microspheres with micro- and nano-scale composite structure self-assembled by nanosheets were successfully fabricated by the template-free wet-chemical approach. This method is simple, facile and effective. The Co_3O_4 hollow microspheres with good purity and homogeneous size were well characterized by scanning electron microscopy (SEM), transmission electron microscopy (TEM), X-ray diffraction (XRD), Fourier transform IR (FTIR), thermogravimetric analysis (TGA) and inductively coupled plasma atomic emission spectrometer (ICP). The formation mechanism was deeply studied. The micro- and nano-scale composite structure constructed by the porous nanosheets promotes to improve the electrochemical properties of Co_3O_4 hollow microspheres. The high discharge capacity of 1048 mAh g^{-1} indicates it to be the potential application in electrode materials of Li-ion battery.

1. Introduction

In the past 15 years or so, various synthesis methods for a wide range of nanoparticles with different shapes were established [1–6]. In recent years, many efforts have been focused on assembling one-dimensional (1-D) nanoscale building blocks into two- and three-dimensional (2-D and 3-D) ordered superstructures or complex functional architectures, which is a crucial step toward the realization of functional nano-devices [7]. However, in addition to common 1-, 2-, and 3-D architectures, controlled organization of primary building units into curved structures represents another challenge for exploiting new functional materials, because hollow structures are highly demanded in new technological applications [8–12].

Spinel Co_3O_4 is an important functional material for a wide range of technological applications such as heterogeneous catalysts, anode materials in Li-ion rechargeable batteries, solid-state sensors, magnetism, and optical devices [13–23]. Owing to the influence of particle size and morphology on the properties of materials, the controlled preparation of Co_3O_4 particles of different sizes and morphologies is always the researcher's purpose. Up to now, Co_3O_4 particles with various morphologies, such as nanotubes [13], nanorods [13], nanosheets [14], hollow nanospheres [15] and nanocubes [16], have been prepared. However, few literatures have been reported on micro- and nano-scale composite Co_3O_4 hollow microspheres with high purity and homogeneous size.

In this paper, we describe a facile template-free wet-chemical approach [24,25] to fabricating Co_3O_4 hollow microspheres with micro- and nano-scale composite structure self-assembled by nanosheets. In the reaction system, cobalt chloride is used as cobalt source and ethylene glycol (EG) as solvent. The hollow spherical intermediate complex (Co–EG coordination polymer) was obtained first by the wet-chemical method. After annealing at 500 °C for 20 min under air, Co_3O_4 hollow microspheres with the similar morphology were formed (see experimental section for the details). Electrochemical results indicate that Co_3O_4 hollow microspheres as the electrode material of Li-ion battery have the high discharge capacity of 1048 mAh g^{-1}.

2. Experimental section

$CoCl_2 \cdot 6H_2O$ (0.7138 g, 3 mmol) was dissolved in EG (24 mL) to form a transparent solution, and then sodium acetate (CH_3COONa, NaAc) (2.16 g) and polyethylene glycol 200 (PEG200) (0.6 g) were added into the above solution. The mixed solution was stirred and gradually became transparent, and then sealed in a Teflon-lined stainless-steel autoclave (30 mL capacity). The autoclave was heated to and maintained at 180 °C for 12 h, and allowed to cool to

* Corresponding author. Fax: +86 25 83314502.
E-mail address: zhengxu@netra.nju.edu.cn (Z. Xu).

0022-4596/$ - see front matter © 2009 Elsevier Inc. All rights reserved.
doi:10.1016/j.jssc.2009.01.030

room temperature. The peach products were collected and rinsed more than five times by ethanol, and dried at 60 °C for 5 h, which was the intermediate complex of Co_3O_4 hollow microspheres. After the peach product was annealed at 500 °C for 20 min, Co_3O_4 hollow microspheres were obtained.

The as-prepared samples were characterized by transmission electron microscopy (TEM), high-resolution transmission electron microscopy (HRTEM) and fast Fourier transform (FFT) (Fecnai G^2 20 S-TWIN from FEI Corporation, 200 kV), energy dispersive X-ray (EDX, GENESIS2000 XMS from EDAX corp. 200 kV), scanning electron microscopy (SEM, JEOL JSM-5610 LV SEM, 20 kV), X-ray diffraction (XRD, D/Max-RA diffractometer, Cu$K\alpha$ radiation), Fourier transform IR (FTIR, VECTOR 22 from BRUKER), thermogravimetric analysis (TGA, LABSYS from SWTERAM), and inductively coupled plasma atomic emission spectrometer (ICP, JA1100 from Jarrell-Ash Corp.).

Co_3O_4 electrode was prepared by coating an active paste into aluminum foil. A paste contained 80 wt% Co_3O_4, 10 wt% carbon black, and 10 wt% polytetrafluoroethylene (PTFE). The coated electrode was placed in vacuum at 100 °C for at least 8 h. Electrochemical performance was measured on Roofer Battery Tester from ShenZhen, China, under labconco glovebox protected by argon gas in electrochemical cell of two electrodes, which contained the cobalt oxide working electrode and lithium counter

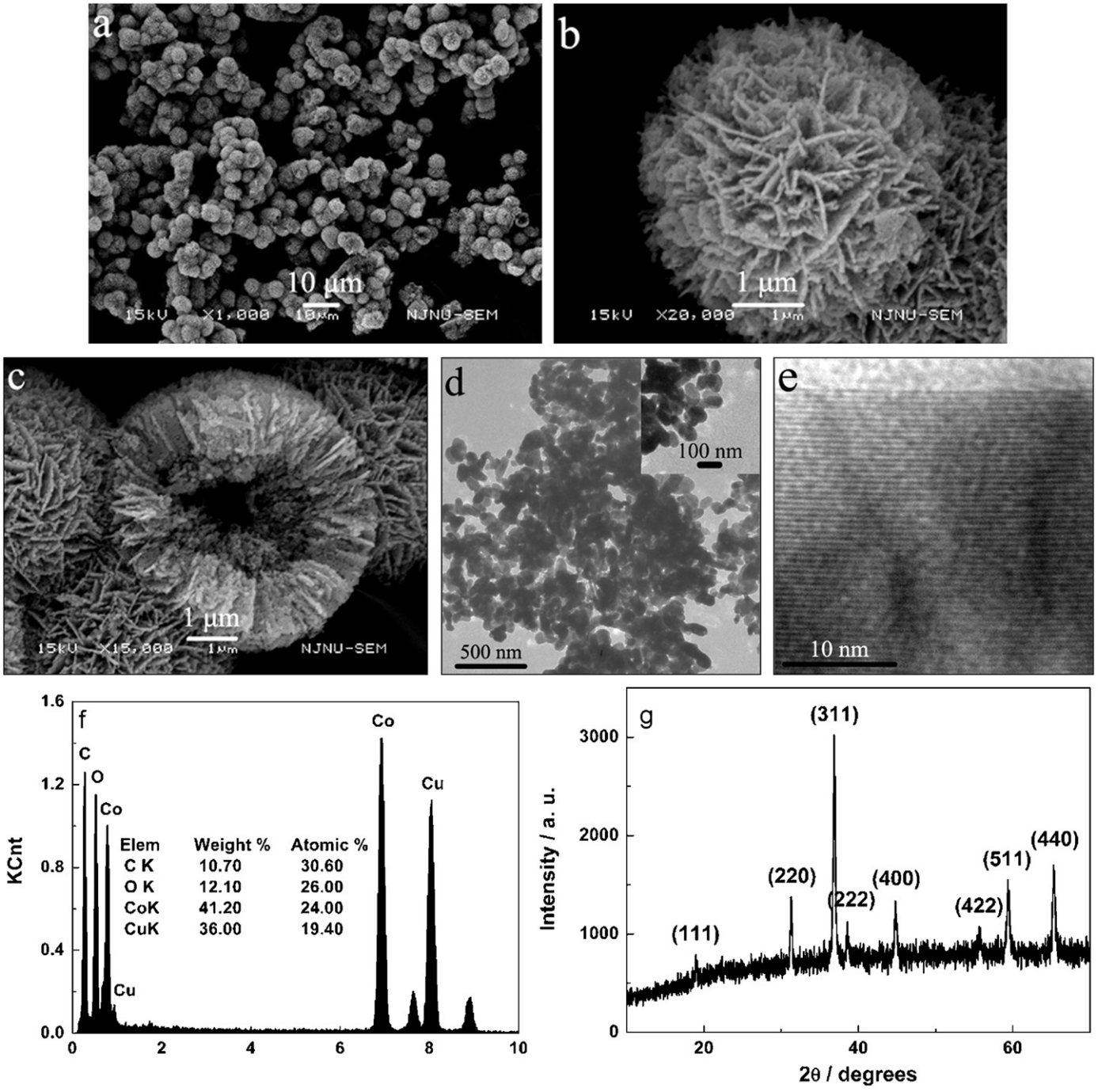

Fig. 1. SEM images (a–c) of Co_3O_4 hollow microspheres: (a) the low magnification, (b) a whole microsphere, and (c) a broken microsphere. TEM (d) and HRTEM images (e) of a nanosheet constructing Co_3O_4 hollow microspheres, and the inset in Fig. 1d shows the TEM image of the verge of a nanosheet. EDX analysis (f) and XRD pattern (g) of Co_3O_4 hollow microspheres.

electrode. The electrolyte solution was 1 M $LiPF_6$ dissolved in a mixture of ethylene carbonate (EC), dimethyl carbonate (DMC), and diethyl carbonate (DEC) with the volume ratio of EC:DMC:DEC = 1:1:1. Charge–discharge cycles were tested with a current density of 0.2 mA cm^{-2} in the potential range 3.0–0.1 V at the temperature of 25 °C.

3. Results and discussion

Fig. 1a–c shows the scanning electron microscopy (SEM) images of Co_3O_4 hollow microspheres with the size range of 3–7 μm, indicating the homogeneous size and high purity of the product. Fig. 1c clearly shows that the product is hollow microspheres composed of interweaving nanosheets, which are orderly aligned perpendicularly to the spherical surface. The shell thickness is about one-fourth or one-third of the diameter of the microspheres. TEM image of single nanosheet constructing Co_3O_4 hollow microspheres in Fig. 1d shows that the nanosheets are composed of small particles of ~50 nm, leading to the porous surface of nanosheets as shown in the inset of Fig. 1d. FFT result from Fig. 1e proves the crystal lattice fringes of 0.46 nm, corresponding to the distance of the adjacent (111) planes of face-centered cubic (fcc) Co_3O_4. Energy-dispersive X-ray (EDX) analyses in Fig. 1f show the existence of Co, O, Cu, and C elements. The atom ratio of Co and O is 1:1.08, which approaches the Co_3O_4 theoretical value. Cu and C elements come from the carbon-coated copper grid. XRD pattern of Co_3O_4 hollow microspheres in Fig. 1g shows that all recorded peaks can be assigned to face-centered cubic (fcc) Co_3O_4 phase in good agreement with JCPDS no. 43-1003. No peaks from other phases are found, suggesting high purity of Co_3O_4 hollow microspheres and also, the product being completely transformed into Co_3O_4 after annealing at 500 °C. Calcination treatment hardly changes the morphology of the final products as shown in Fig. 5d, indicating the good thermal stability of Co_3O_4 composite structure. Therefore, we mainly discuss the effect of experimental parameters on the morphologies of Co_3O_4 intermediate products.

The Co–EG coordination polymer, the intermediate product of Co_3O_4 hollow microspheres fabricated at 180 °C for 12 h, was proved by XRD, FTIR spectrum, TGA pattern, and ICP, respectively. A strong diffraction peak around 10° in XRD pattern shown in Fig. 2 is the characteristic one of the coordination polymer composed of metal ions and EG [26,27]. In FTIR spectrum in Fig. 3, the absorption peaks at 2850 and 1084 cm^{-1} are attributed to C–H and C–O stretching vibration modes, proving the existence of EG in the intermediate product. TGA curve shown in Fig. 4 indicates that there is a rapid weight loss from 300 to 350 °C, followed by a slower weight loss process up to about 500 °C. The total weight loss below 500 °C is about 31.5 wt%, in good agreement with the theoretical value of 32.5 wt% by losing one EC and forming Co_3O_4. In addition, ICP result shows 48.1 wt% of Co content in good agreement with the theoretical value of 49.6 wt%. It further indicates that the intermediate product of Co_3O_4 hollow microspheres is the coordination polymer composed of one EC molecule and one cobalt ion.

To get an insight into the formation mechanism of Co_3O_4 hollow microspheres with micro- and nano-scale composite structure, time-dependent experiments were carried out and the intermediate products were inspected by SEM. The images were shown in Fig. 5, from which the evolution process can be clearly seen. At the beginning of the reaction, only smooth solid microspheres with the uniform size of about 3 μm were formed after reacting for 4 h in Fig. 5a. With the increasing reaction time to 6 h, the microspheres became a little bigger and rough, and the inner slowly dissolved as shown in the top inset of Fig. 5b.

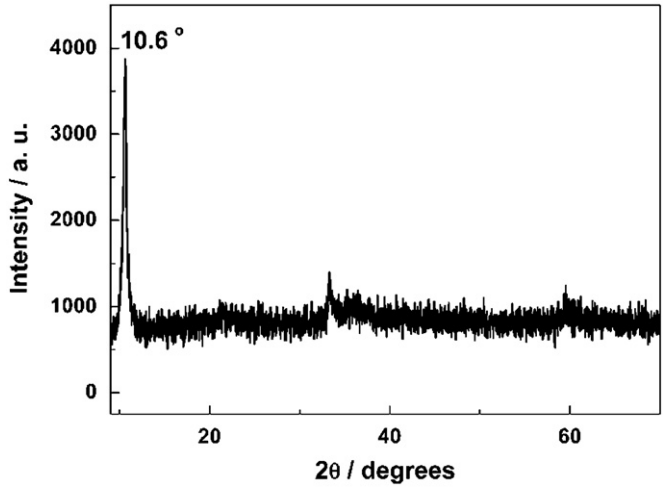

Fig. 2. XRD pattern of the intermediate product of Co_3O_4 hollow microspheres.

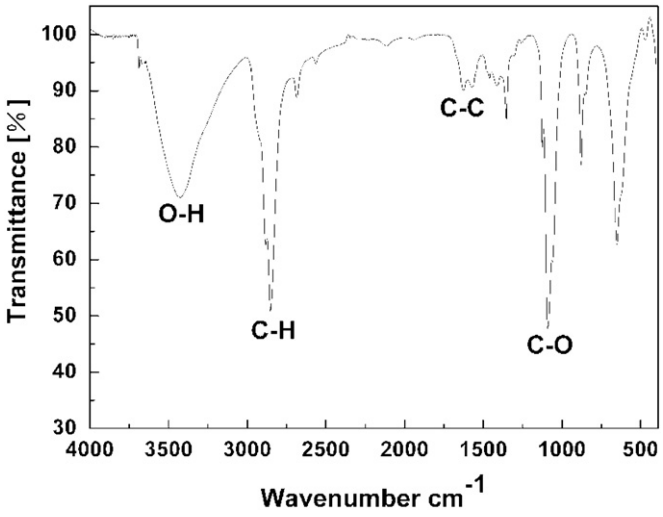

Fig. 3. FTIR spectrum of the intermediate product of Co_3O_4 hollow microspheres.

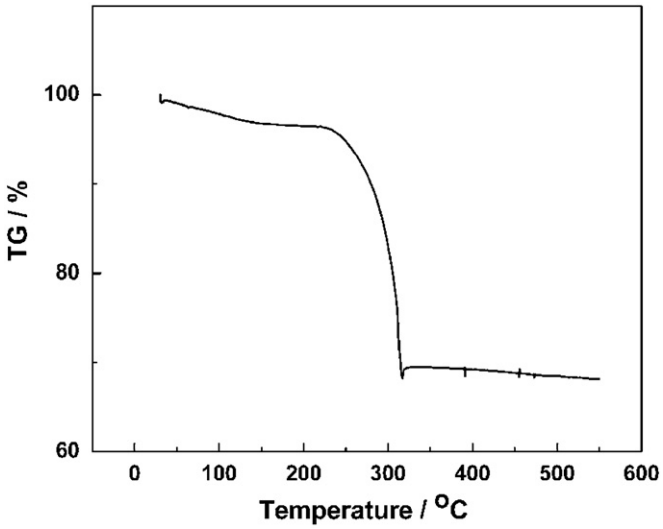

Fig. 4. TGA curve of the intermediate product of Co_3O_4 hollow microspheres.

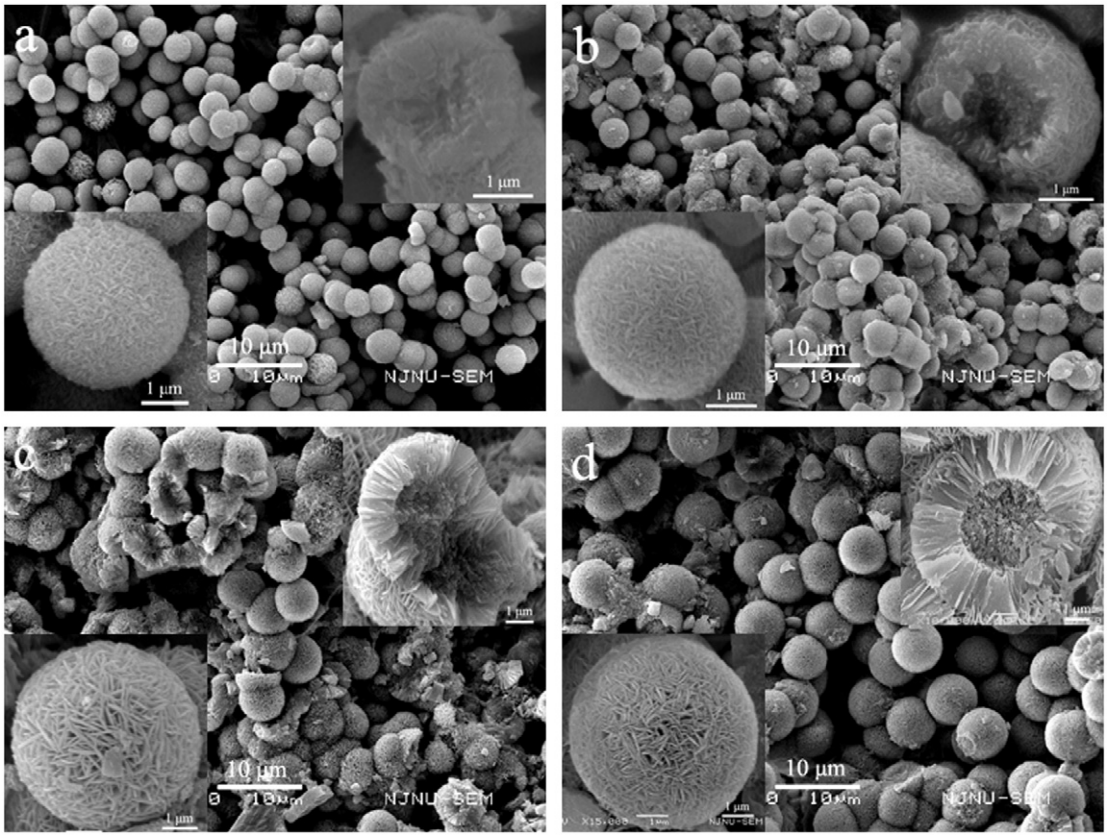

Fig. 5. SEM images of the intermediate products of Co_3O_4 at the different reaction times: (a) 4 h, (b) 6 h, (c) 8 h, and (d) 12 h. The insets of Fig. 5a–d at right top and left bottom show the SEM images of the broken and the whole microspheres in corresponding photos, respectively.

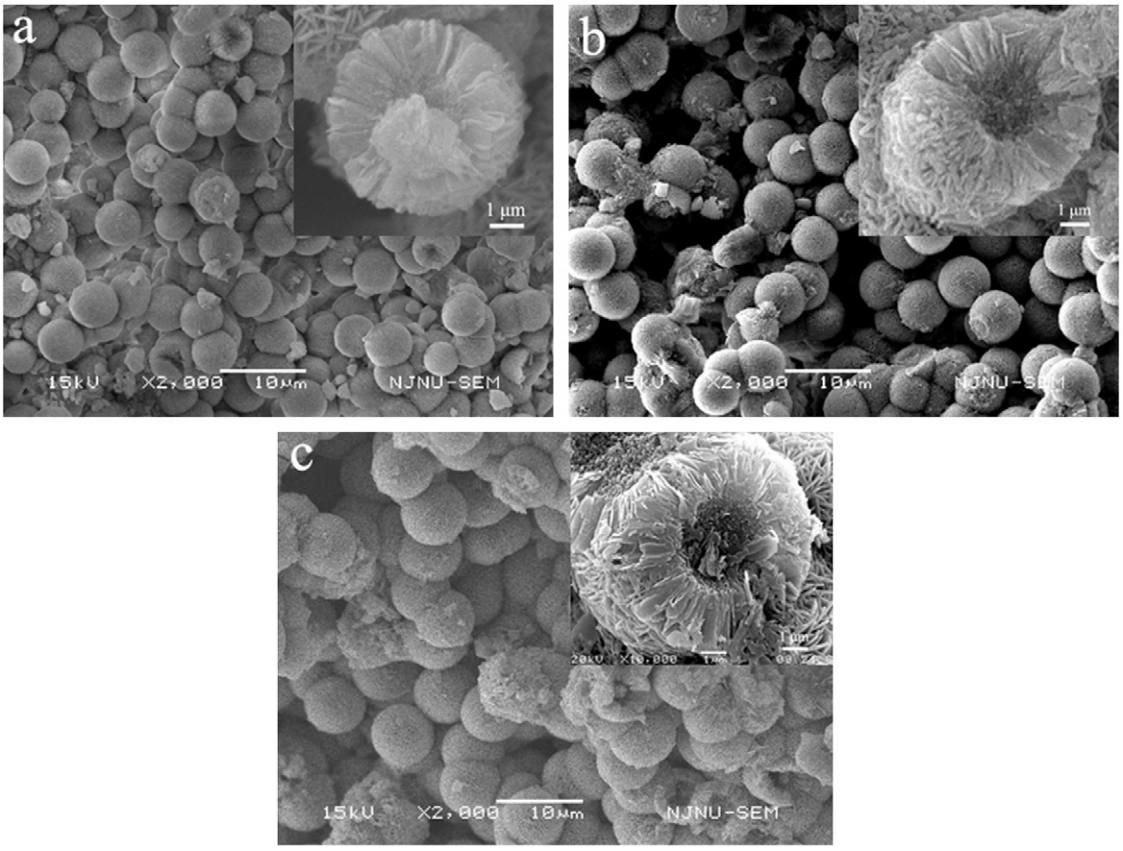

Fig. 6. SEM images of the intermediate products of Co_3O_4 at the different concentration of polyethylene glycol 200 (PEG200): (a) 0 g L^{-1}, (b) 8.3 g L^{-1}, and (c) 62.5 g L^{-1}. The top insets of Fig. 6a–c show the SEM images of the broken microspheres in corresponding photos, respectively.

After reacting for 8 h in Fig. 5c, the microsphere size increased up to about 5 μm and the length of the nanosheets was about 1 μm. The diameter of hollow part of about 3 μm was consistent with that of solid sphere in Fig. 5a, indicating that the nanosheets grew up on the microsphere surface, and the microspheres slowly dissolved from the inner, and finally the hollow microspheres composed of nanosheets were formed. After the reaction for 12 h in Fig. 5d, the uniform hollow microspheres self-assembled by nanosheets of about 1.5 μm were finally formed. The above experimental results clearly indicate that the formation of hollow microspheres is a dissolution-recrystallization process. In the ripening process, the nanosheets first nucleate and grow on the surface of solid microspheres, which prevents further dissolution of surface layer of solid spheres and promotes the transportation of inner core to outer surface and the formation of larger hollow microspheres self-assembled by nanosheets as shown in Fig. 5d.

Based on the plentiful experiments, it is found that polyethylene glycol 200 (PEG200) plays an important role in the formation process of Co_3O_4 hollow microspheres. Therefore, we lay a strong emphasis on the effect of the concentration of PEG200 on the morphologies of the intermediate products in Fig. 6 and on the relation of reaction time with the morphologies of the products without PEG200 in Fig. 7. The SEM images in Fig. 6 indicate that the formation of the hollow microsphere is dependent on the presence of PEG200, but is less relative with the concentration of PEG200 (in the range of 8–250 g L^{-1}). Without PEG200, only solid microspheres composed of nanosheets were obtained as shown in Fig. 6a. To get further information, the time-dependent experiments were performed without PEG200. From the SEM images in Fig. 7, it was found that at the reaction time of 4 h the microspheres were still solid and about 3 μm in diameter. As the reaction time increasing, the nanosheets nucleated on the surface of solid spheres and grew up, but the solid structures keep constant. Finally, the solid microspheres self-assembled by the interweaving nanosheets were formed, similar to that in Fig. 5.

Based on the above experimental results, we may consider that at the first stage of reaction the reaction products with and without PEG200 have no obvious difference in apparent morphology, and both of them are the solid microspheres. However, when PEG200 is present, PEG200 might enter into the initial product because of the similar structure and composition with EG. It makes the initial solid spheres loose structure and is favorable for the dissolution of the inner part of solid microspheres and the formation of the hollow microspheres composed of nanosheets at the second stage of the reaction, that is ripening process. Whereas the absence of PEG200 in the reaction system, the initial product is tightly packed in the solid microspheres, which prevents the inner part from dissolving. The solid structure is remained as the core and the interweaved nanosheets grow up on the core surface to form the core-shell structure.

In addition, sodium acetate (CH_3COONa, NaAc) also plays an important role in the formation of the hollow microspheres composed of nanosheets. The experimental results show that the formation of hollow microspheres is very sensitive to the concentration of NaAc. There is an optimum concentration range of 0.38–1.52 mol L^{-1}. The lower (less than 0.38 mol L^{-1}) and higher concentration (greater than 1.52 mol L^{-1}) will only form nanosheets rather than the hollow microspheres. In addition, reaction temperature has an effect to some extent on the morphology of the reaction product. The reaction temperature higher than 180 °C leads to the formation of similar hollow microspheres composed of the disorder array of nanosheets and at the lower temperature there is not any product.

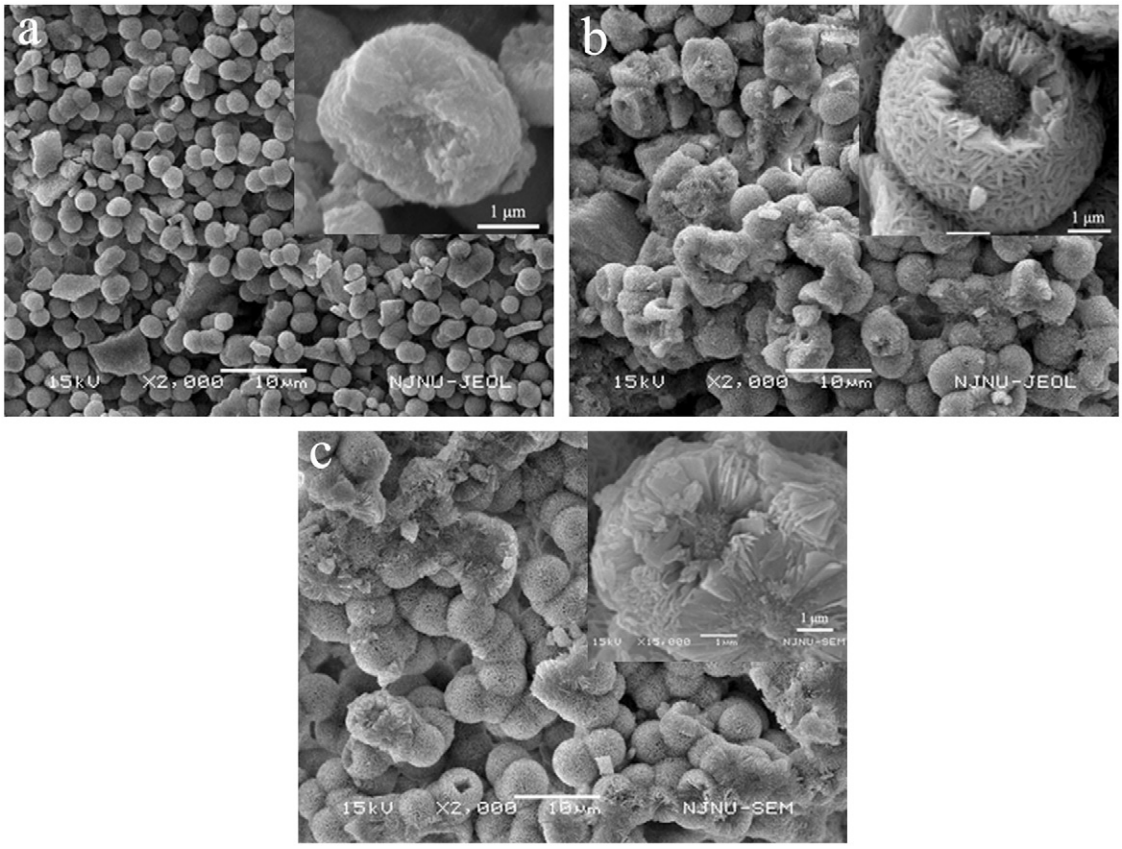

Fig. 7. SEM images of the intermediate products of Co_3O_4 without the polyethylene glycol 200 (PEG200), (a) 4 h, (b) 6 h, and (c) 9 h. The top insets of Fig. 7a–c show the SEM images of the broken microspheres in corresponding photos, respectively.

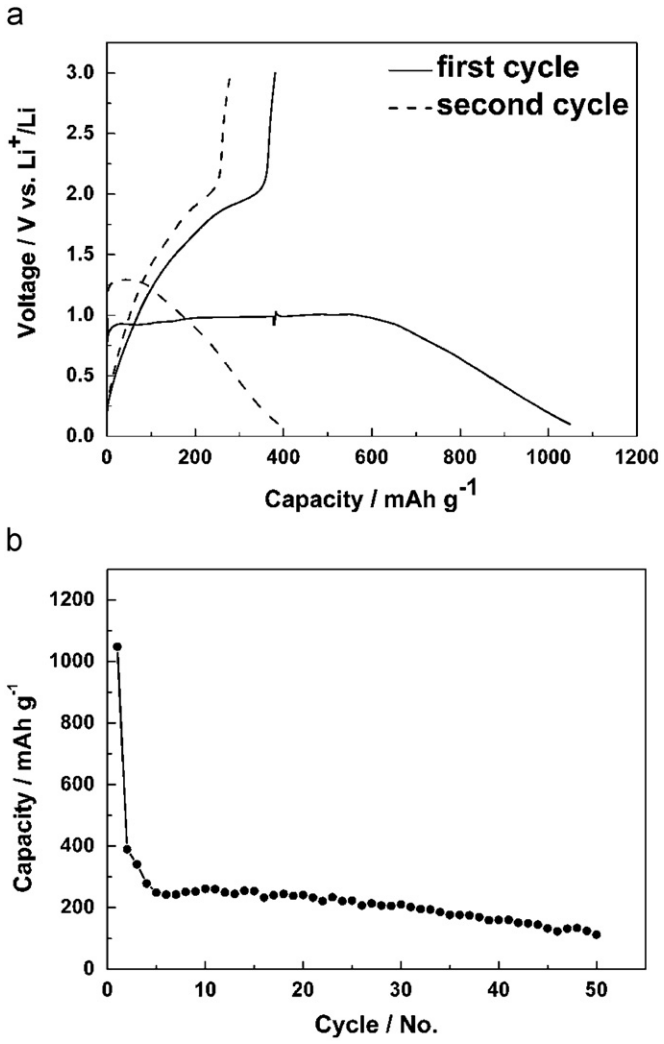

Fig. 8. (a) Discharge curves: first cycle (solid line) and second cycle (dashed line) and (b) the plot of capacity versus cycle no. for Co_3O_4 hollow microspheres composed of nanosheets.

Co_3O_4 is a good electrode material for Li-ion battery and has the strong electron storage ability. The novel Co_3O_4 hollow microspheres composed of porous nanosheets might be a good candidate of electrode material. As shown in Fig. 8a, the discharge capacity of the hollow microspheres in the first cycle is 1048 mAh g^{-1}, which is about 200 mAh g^{-1} higher than one reported in the literature [13]. The significantly improved discharge capacity of Co_3O_4 hollow microspheres may be attributed to its unique morphology. The porous nanosheets constructing Co_3O_4 hollow microspheres are favorable for increasing the interface area between electrode and electrolyte, which can result in a higher diffusion rate and faster electrode kinetics, and also can increase the usage factor of the active component of the electrode. Therefore, Co_3O_4 hollow microspheres with micro- and nano-scale composite structure have high discharge capacity. However, the discharge capacity rapidly decreases to 390 mAh g^{-1} at the second cycle, indicating its poor stability. The further study is needed to improve this.

4. Conclusion

The Co_3O_4 hollow microspheres composed of nanosheets were successfully fabricated by the template-free wet-chemical method. The effect of the experimental parameters on the formation of Co_3O_4 hollow microspheres with micro- and nano-scale composite structure was studied by SEM, TEM, HRTEM, XRD, FTIR, TGA, and ICP. The possible formation mechanism was suggested. Co_3O_4 hollow microspheres as the electrode material of Li-ion battery have the high discharge capacity of 1048 mAh g^{-1}, which is 200 mAh g^{-1} higher than one reported in the literature [13]. It might be a potential candidate for electrode materials of Li-ion battery. However, Co_3O_4 hollow microspheres have a poor electrochemical stability and the further improvement is needed.

Acknowledgments

We acknowledge financial support from the National Natural Science Foundation of China (NSFC) under major research programmer of nanoscience and nanotechnology no. 90606005, major programmer no. 20490210, and project no. 20571040.

References

[1] L. Manna, E.C. Scher, A.P. Alivisatos, J. Am. Chem. Soc. 122 (2000) 12700.
[2] S.-M. Lee, Y.-W. Jun, S.-N. Cho, J. Cheon, J. Am. Chem. Soc. 124 (2002) 11244.
[3] Y. Sun, Y. Xia, Science 298 (2002) 2176.
[4] J. Goldberger, R. He, Y. Zhang, S. Lee, H. Yan, H.-J. Choi, P. Yang, Nature 422 (2003) 599.
[5] H.Y. Koo, W.S. Choi, J.-H. Park, D.-Y. Kim, Macromol. Rapid Commun. 29 (2008) 520.
[6] J. Zhang, L. Wang, D. Pan, S. Song, F.Y.C. Boey, H. Zhang, C. Fan, Small 4 (2008) 1196.
[7] Y. Huang, X.F. Duan, Q.Q. Wei, C.M. Lieber, Science 291 (2001) 630.
[8] F. Caruso, R.A. Caruso, H. Möhwald, Science 282 (1998) 1111.
[9] B. Liu, H.C. Zeng, J. Am. Chem. Soc. 126 (2004) 8124.
[10] B. Liu, H.C. Zeng, J. Am. Chem. Soc. 126 (2004) 16744.
[11] X. Li, Y. Xiong, Z. Li, Y. Xie, Inorg. Chem. 45 (2006) 3493.
[12] D. Chen, J. Ye, Adv. Funct. Mater. 18 (2008) 1922.
[13] W.-Y. Li, L.-N. Xu, J. Chen, Adv. Funct. Mater. 15 (2005) 851.
[14] E. Hosono, S. Fujihara, I. Honma, H. Zhou, J. Mater. Chem. 15 (2005) 1938.
[15] H. Yoshikawa, K. Hayashida, Y. Kozuka, A. Horiguchi, K. Awaga, S. Bandow, S. Iijima, Appl. Phys. Lett. 85 (2004) 5287.
[16] R. Xu, H.C. Zeng, Langmuir 20 (2004) 9780.
[17] C.-H. Chen, S.F. Abbas, A. Morey, S. Sithambaram, L.-P. Xu, H.F. Garces, W.A. Hines, S.L. Suib, Adv. Mater. 20 (2008) 1205.
[18] F. Teng, W. Yao, Y. Zheng, Y. Ma, T. Xu, G. Gao, S. Liang, Y. Teng, Y. Zhu, Talanta 76 (2008) 1058.
[19] M. Ohnishi, Y. Kozuka, Q.-L. Ye, H. Yoshikawa, K. Awaga, R. Matsuno, M. Kobayashi, A. Takahara, T. Yokoyama, S. Bandow, S. Iijima, J. Mater. Chem. 16 (2006) 3215.
[20] F. Teng, T. Xu, S. Liang, G. Buergen, W. Yao, Y. Zhu, Catalysis Comm. 9 (2008) 1119.
[21] A.-M. Cao, J.-S. Hu, H.-P. Liang, W.-G. Song, L.-J. Wan, X.-L. He, X.-G. Gao, S.-H. Xia, J. Phys. Chem. B 110 (2006) 15858.
[22] P. Poizot, S. Laruelle, S. Grugeon, L. Dupont, J.-M. Tarascon, Nature 407 (2000) 496.
[23] K.T. Nam, D.-W. Kim, P.J. Yoo, C.Y. Chiang, N. Meethong, P.T. Hammond, Y.-M. Chiang, A.M. Belcher, Science 312 (2006) 885.
[24] L.-P. Zhu, H.-M. Xiao, W.-D. Zhang, G. Yang, S.-Y. Fu, Cryst. Growth Des. 8 (2008) 957.
[25] X.W. Lou, Y. Wang, C. Yuan, J.Y. Lee, L.A. Archer, Adv. Mater. 18 (2006) 2325.
[26] X. Jiang, Y. Wang, T. Herricks, Y. Xia, J. Mater. Chem. 14 (2004) 695.
[27] Y. Wang, X. Jiang, Y. Xia, J. Am. Chem. Soc. 125 (2003) 16176.